

A thermal micro pressure sensor: its characteristics and application to pressure measurement in a minute package

Non-member	Shinan Wang	(Toyota Central R & D Labs., Inc.)
Non-member	Kentaro Mizuno	(Toyota Central R & D Labs., Inc.)
Member	Motohiro Fujiyoshi	(Toyota Central R & D Labs., Inc.)
Non-member	Hirofumi Funabashi	(Toyota Central R & D Labs., Inc.)
Non-member	Jiro Sakata	(Toyota Central R & D Labs., Inc.)

A thermal micro pressure sensor suitable for measurement in the range of 7×10^{-3} to 1×10^5 Pa was realized by forming a titanium (Ti) thin-film resistor on a floating NSG (non-doped silica glass) membrane, with the sensing area being as small as $60 \mu\text{m} \times 60 \mu\text{m}$. The sensor performance was raised by increasing the gaseous ratio to the total thermal conduction, compensating the effect of ambient-temperature drift, and utilizing an optimized novel constant-bias Wheatstone bridge circuit. The sensor was successfully applied to monitoring the pressure in a sealed minute metal package with a capacity of about 0.5 ml.

Keywords: micro pressure sensor, thermal conduction, constant-bias circuit, pressure sensing in minute package

1. Introduction

Sensors and actuators in micro sizes, which may have overwhelming advantages in such as functions and cost compared to conventional macro ones, have been taken for granted nowadays due to the remarkable development of micromachining technologies. However, when a device gets down to micro sizes, effects such as friction, sticking and air damping become notable and sometimes may determine the device characteristics. For example, the resonant amplitude and half-value width of a micro oscillator depend strongly on the ambient air pressure due to dumping effect, which has been used to detect gas pressure. It is then necessary to package the device under a steady pressure (usually a reduced pressure to obtain satisfactory performance) when the oscillator is used for purposes other than pressure sensing. This directly demands the precise detection of pressure and pressure steadiness in the sealed minute package, which calls for a micro pressure sensor with high resolution and especially, micro sizes.

Various micro sensors have been developed and proposed for pressure detection and may be roughly classified as follows: (i) The aforementioned resonant type⁽¹⁾. One of its shortages is the low sensitivity in pressure regime lower than 1Pa. (ii) The ionization gauge⁽²⁾. It is expected to be suitable for ultrahigh vacuum measurement. However, since electrons emitted from a cathode must be sufficiently accelerated to collide with and ionize gas molecules, a high voltage circuit and a relatively large device size are always necessary. (iii) The mechanical type. A thin

diaphragm is usually used and its deformation caused by pressure difference between the target and the standard pressures is detected by measuring the corresponding change in such as electrostatic capacity⁽³⁾, piezoelectric resistance⁽⁴⁾ or optical quantities⁽⁵⁾. The fatal disadvantage of this kind of sensors is the necessity of a vacuum room to supply the pressure standard, whose reliability is also to be evaluated. (iv) The thermal type (the Pirani type)^(6,7). The principle is simple: when gas molecules collide with the heated sensing part, heat is taken away in a quantity depending on the molecule numbers, and therefore the gas pressure. Compared to other pressure sensors, the thermal type is superior in possibilities of small size, easy-to-fabricate simple structure and above all, high resolution and wide range. In this work, the thermal sensor is showed a good candidate for high-resolution pressure measurement in a minute package.

2. Sensor Fabrication

The sensor was fabricated by micromachining techniques. A photograph of the sensing part is illustrated in Fig. 1. A schematic of the sensor is illustrated in Figs. 2 a (top view) and b (cross-sectional view). The element is composed of a titanium (Ti) thin-film (80nm thick) resistor (R_s) patterned into a square-wave structure and sandwiched by two NSG (non-doped silica glass) thin films (350nm thick each). In order to realize good thermal insulation of solid conduction, the sensing part is cut away from the substrate by a conventional silicon (Si) anisotropic etching method⁽⁸⁾, leaving only four narrow beams to support the $60 \mu\text{m} \times 60 \mu\text{m}$ floating membrane. The NSG

membrane not only supports the Ti resistor but also protects it from oxidation. The solid thermal conduction, with the beams as its only paths, is extremely reduced by the low thermal conductivity of NSG and the thin beam design: 0.78 μm thick, 65 μm long and as narrow as 4 μm . A reference resistor (R_r), also made from Ti, is simultaneously formed directly on the Si substrate (without thermal insulation) to reduce the ambient temperature (T_a) dependence of the sensor characteristics.

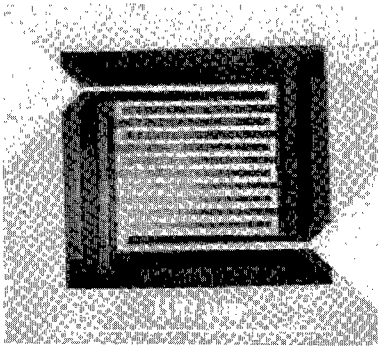
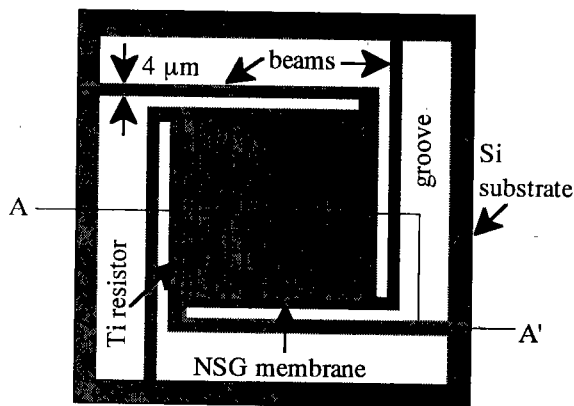
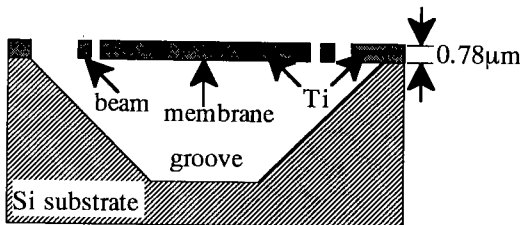


Fig. 1. Top-view photograph of the sensing element of a thermal micro pressure sensor fabricated by micromachining techniques.



a) top view



b) cross-sectional view

Fig. 2. Schematic of the thermal sensor: a) top view, and b) cross-sectional view.

3. Sensor Characteristics

3.1 Thermal Conduction

The heated sensor loses heat Q_T by radiation (Q_r), solid conduction through the beams to the substrate (Q_s), and gaseous conduction to both the backside substrate and the forward ambience (Q_g), which can be simply expressed by Eqs. 1-4:

$$Q_T = Q_r + Q_s + Q_g \quad (1)$$

$$Q_r = \sigma \epsilon (T_s^4 - T_a^4) A_s \quad (2)$$

$$Q_s = K A_b (T_s - T_a) / L \quad (3)$$

$$Q_g = \alpha \Lambda (273 / T_a)^{1/2} (T_s - T_a) A_s P \quad (4)$$

where σ is the Stefan-Boltzmann radiation constant, ϵ and K are the thermal emissivity and thermal conductivity of NSG, α and Λ are the accommodation coefficient and free molecule thermal conductivity of the ambient gas, respectively; A_s is the total surface area of the membrane, A_b is the total cross sectional area of the beams by which they are connected to the substrate, while L is the length of a single beam; T_a is the ambient temperature, T_s is the sensor temperature and P is the ambient gas pressure. For simplicity, only an expression in the free molecular flow regime of Q_g is showed in Eq. 4.

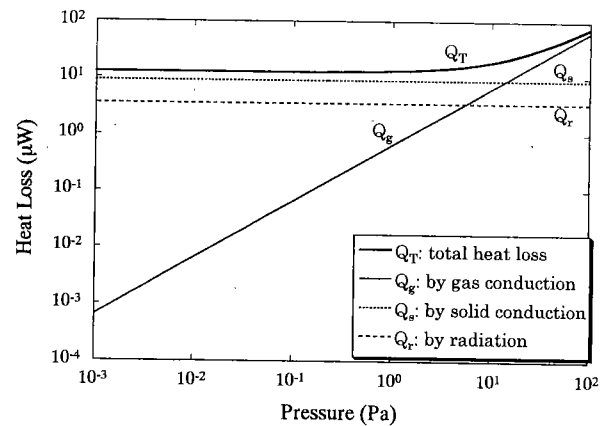


Fig. 3. Calculated heat losses as a function of ambient gas pressure.

The heat losses Q_T , Q_r , Q_s and Q_g are calculated by using Eqs. 1-4 and plotted against P in Fig. 3, where the experimental material and device parameters are adopted while the temperatures are assumed as $T_a=300\text{K}$, $T_s=350\text{K}$. As obviously observed in Fig. 3, only Q_g is gas pressure dependent and a Q_T -based sensor characteristic becomes saturate as $P < 1\text{Pa}$ since Q_g decreases linearly with P and occupies a very small ratio

in Q_T in the low pressure regime. This implies two ways to expand the sensing range and to elevate the resolution. One way is to extend the molecular flow regime[7] and to increase the Q_g/Q_T ratio, which may be realized by proper device structure design basing on the thermal conduction mechanism, but meanwhile, with the experimental permission. Another way is to extract Q_g from Q_T , which requires tricks of electronic circuitry and signal analysis.

3.2 T_a -Dependence of Sensor Characteristics

Like other types, the thermal pressure sensor is ambient-temperature (T_a) dependent. This effect was studied by using a simple Wheatstone bridge circuit with the sensor R_s as one leg of the bridge (inserts of Figs. 4 and 5). In Fig. 4, when a voltage V_o is applied, R_0 and

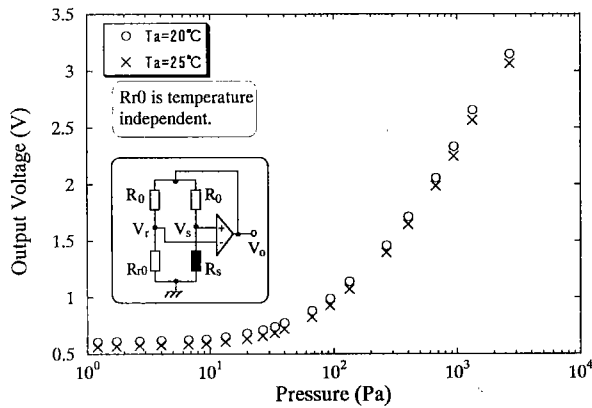


Fig. 4. Sensor characteristics measured by using a simple bridge circuit (the insert), with only the sensor R_s being temperature dependent.

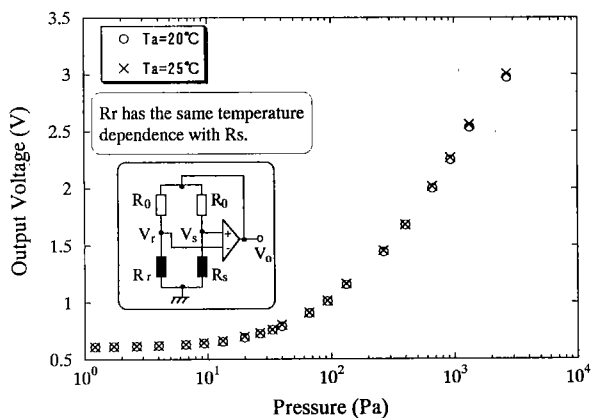


Fig. 5. Sensor characteristics measured by using a simple bridge circuit (the insert), with the reference resistor R_r having the same temperature dependence with the sensor R_s .

R_{r0} keep constant, while R_s is heated to temperature T_s and

$$R_s = R_{sa} [1 + C_T (T_s - T_a)], \quad (5)$$

where C_T is the temperature coefficient of resistance (of Ti, here) and $R_{sa} = R_s (T_s = T_a)$. The circuit operates to keep $V_s = V_r$, namely, $R_s = R_{r0} = \text{constant}$. In such a circuit, V_o is a Q_T -based quantity. Since R_{r0} is chosen in such a way that $R_{r0} = 1.15 \sim 1.36 R_{sa}$ at 30°C (it is the same with R_r), and C_T is measured to be $C_T = 0.3\% \text{K}^{-1}$, the sensor temperature T_s is $50 \sim 120^\circ\text{C}$ above the ambient temperature T_a in thermal equilibrium state.

As showed in Fig. 4, a T_a variation (ΔT_a) leads to a V_o - P curve shift in proportion to $-\Delta T_a$, which directly limits the sensing range and resolution. R_{r0} is then replaced by R_r (insert of Fig. 5), which has the same T_C with R_s . In this case, since R_r is directly located on the Si substrate, a good thermal conductor, its temperature is kept at T_a even when an electric current flows through it. In thermal equilibrium state, $R_s = R_r$, is a quantity depending on T_a . As showed in Fig. 5, the sensor characteristic drift is greatly reduced by the compensation effect of R_r . These results are found in good agreement with theoretical calculations.

3.3 Constant-Bias Circuit

According to the theoretical and experimental results showed in Figs. 3-5, it is obvious that a Q_T -based sensor characteristic has a limited range and a vanishing resolution as $P < 1 \text{Pa}$. Since Q_r and Q_s are independent of pressure and lead to the characteristic saturation in low pressure regime, while Q_T is the directly measurable quantity, subtracting a constant close to $Q_r + Q_s$ from Q_T will help extract information on Q_g . For this purpose, a constant-bias Wheatstone bridge circuit, illustrated in Fig.6, is employed.

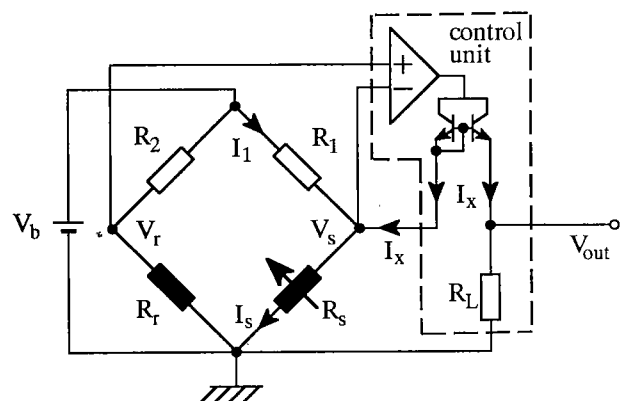


Fig. 6. Constant-bias Wheatstone bridge circuit for high resolution and wide range pressure detection.

In the circuit, a constant bias V_b is applied to the bridge in order to realize the subtraction, and the bridge balance ($V_r=V_s$) is eventually maintained by a control unit that supplies R_s a current I_x . I_x varies corresponding to the gas pressure and is amplified by R_L and detected as the output voltage V_{out} . In Fig. 6,

$$V_{out} = R_L I_x. \quad (6)$$

The current flowing through R_s is

$$I_s = I_1 + I_x. \quad (7)$$

The current flowing through R_1 is

$$I_1 = \frac{V_b - V_s}{R_1}. \quad (8)$$

When the bridge is balanced,

$$I_s R_s = V_s = V_r = \beta V_b, \quad (9)$$

where

$$\beta = \frac{R_r}{R_2 + R_r}.$$

According to Eqs. 7-9, I_x can be expressed as

$$I_x = \frac{V_s}{R_s} - \frac{V_b - V_s}{R_1}. \quad (10)$$

While, the power supplied to R_s by the control unit that balances the bridge is

$$P_s = \frac{V_s^2}{R_s}. \quad (11)$$

Here, we define a quantity S_r as

$$S_r = \frac{R_s - R_{sa}}{R_{sa}} \frac{1}{P_s}. \quad (12)$$

As understood from the equation, S_r is the resistance variation ratio per unit input power, an intrinsic quantity for a given sensor at a fixed ambient temperature. S_r is named as the power sensitivity of resistance and can be found by simple measurement. By using Eqs. 9, 11 and 12, an expression for R_s can be obtained:

$$R_s = \frac{R_{sa}}{2} \left[1 + \sqrt{1 + \frac{4S_r V_b^2}{R_{sa}} \beta^2} \right]. \quad (13)$$

By substituting V_s and R_s in Eq. 10 by those given in equations 9 and 13, respectively, I_x , eventually, V_{out} can be found as

$$V_{out} = R_L I_x = \frac{R_L}{R_1} \left\{ \beta \left[\frac{2R_1 / R_{sa}}{1 + \sqrt{1 + \frac{4S_r V_b^2}{R_{sa}} \beta^2}} + 1 \right] - 1 \right\} V_b. \quad (14)$$

A S_r - P curve measured at 30°C is showed in Fig. 7. The curve indicates that the power sensitivity of resistance is high in the pressure range of $1\text{Pa} < P < 10^4\text{Pa}$, but poor in the two extremes.

The bias voltage V_b dependence of the output signal V_{out} is then calculated by using Eq. 14 and the measured S_r showed in Fig. 7. The result is depicted in Fig. 8. In the calculations, parameters are specified by the same values used in the experiments, as:

$$R_1 = R_2 = R_L = 10 \text{ k}\Omega$$

$$R_r = 7.21 \text{ k}\Omega, \text{ at } 30^\circ\text{C}$$

$$R_{sa} = 5.29 \text{ k}\Omega, \text{ at } 30^\circ\text{C}$$

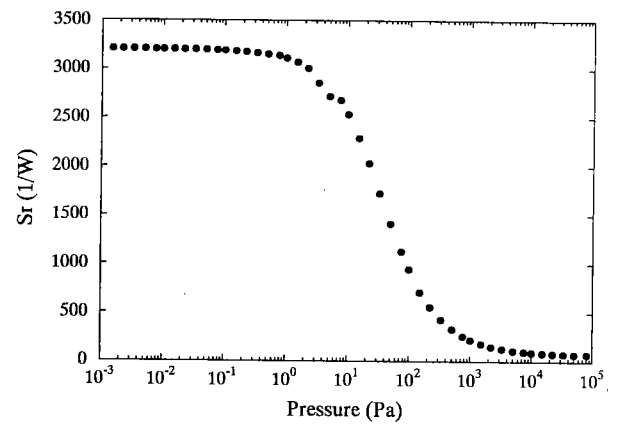


Fig. 7. Measured power sensitivity of resistance versus pressure, of a thermal micro pressure sensor.

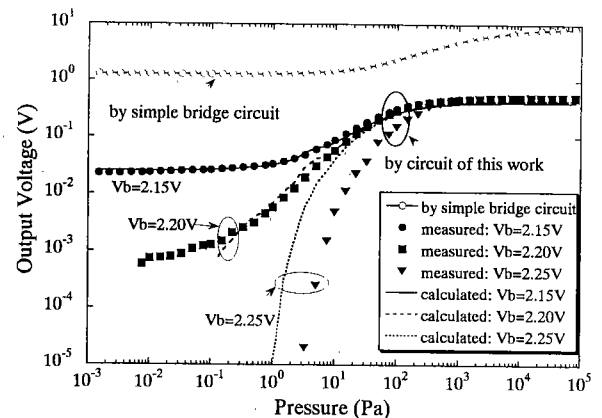


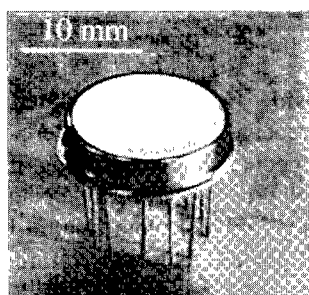
Fig. 8. Calculated and measured sensor characteristics by using the constant-bias circuit showed in Fig. 6. That measured by a simple bridge circuit (insert of Fig. 5) is also displayed for comparison.

It is found from Fig. 8 that the sensor characteristic depends on V_b strongly, with a value of $V_b = 2.20\text{V}$ being the best for the wide range and high resolution purpose in this case. The theoretical prediction is straightforwardly verified by experimental results showed in the figure by black markers. The good agreement between theory and experiment clearly indicates that the optimum V_b value can be derived from Eq. 14. In fact, all circuit parameters can be optimized in the same way.

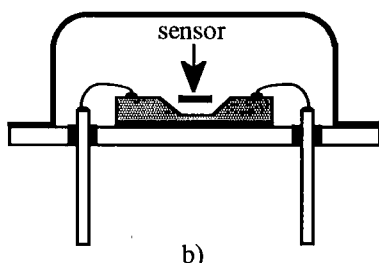
For comparison, a V_o - P curve obtained by the simple Wheatstone bridge circuit (insert of Fig. 5) is also plotted in the figure. Obviously, the sensor characteristic is greatly improved by extracting information on Q_g with the help of the optimized constant-bias circuit.

4. Pressure Sensing in a Minute Package

The micro sensor and the optimized constant-bias circuit are then applied to the pressure measurement in a minute package. First, the sensor was fixed to a metal base (TO-8) by low-melting-point solder and was bonded to the feedthrough pins by aluminum thin wires. The sensor was then calibrated at 30°C in a vacuum chamber filled with N_2 gas. The chamber pressure was read by a MKS digital convection enhanced Pirani gauge (Series 947) in the range of $10\text{Pa} < P < 10^5\text{Pa}$, and by an



a)



b)

Fig. 9. A sealed minute package: a) photograph, b) schematic of the package cross section.

ANELVA digital wide range ionization vacuum sensor (M-430HG-J) in the range of $P < 10\text{Pa}$. The output signal V_{out} was read by a HP 3456A digital voltmeter. Subsequently, the sensor-mounted TO-8 base was sealed with a steel cap by projection welding method, under a reduced pressure. Figures 9 a and b are respectively a photograph of the sealed package and a schematic of its cross section. The capacity of the package is as small as about 0.5ml . Finally, the package was kept in a thermostat at 30°C and the interior pressure P_{in} was detected by reading V_{out} . The obtained time dependence of P_{in} is given in Fig. 10.

For the package showed in Fig. 10, P_{in} increases dramatically from 160Pa to 290Pa in the first 50 hr after sealing, and then gradually tends to increase at a constant rate of $\sim 0.04\text{Pa/hr}$. The initial rapid increase of P_{in} may be due to the degassing of the package inner walls, the sensor and the solder, and will be reduced by baking the package set in vacuum at above 100°C before welding. The later linear increase of P_{in} with time suggests a sealing leakage.

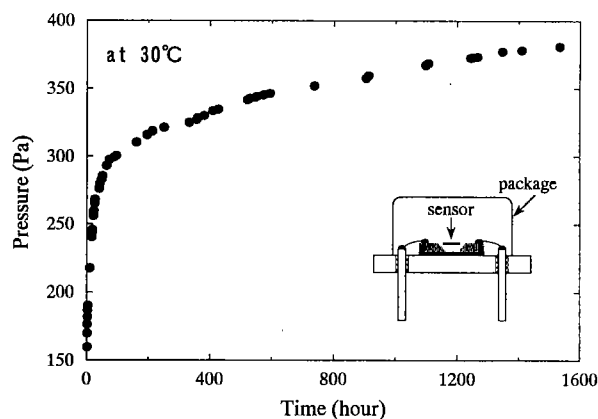


Fig. 10. Pressure in a sealed minute package detected by the thermal micro pressure sensor.

By two methods, the sensor characteristics were proved almost unchanged by sealing and preserving in the sealed package for a long period of time: One method is monitoring the values of C_T , R_s and R_r at 30°C . The other method is to open the package gently and recalibrate the sensor.

5. Discussion and Conclusion

The sensing extremes of thermal micro pressure sensors have been well explored^(6,7). In Ref. 6, by stabilizing the substrate temperature to an accuracy of $\pm 0.001^\circ\text{C}$ and by employing a well-developed circuit, the computer-assisted system is capable of measuring a

pressure as low as 10^{-5} Pa. On the other hand, by creating a heat sink as close as a few μm to the heated sensing part, the molecular flow regime is extended and the sensible upper extreme is extended up to 10^6 Pa⁽⁷⁾. These results present the great potentials of thermal pressure sensors. However, a low cost, easy-to-create simple system is often desirable in practice.

In this work, by using a simple micro sensing element and a novel circuit designed according to the thermal conduction principles, satisfactory sensor performance was obtained in spite of the system simplicity. Such a sensor is showed practically useful for pressure detection in a minute package.

Acknowledgment

The authors thank Mr. N. Fujitsuka, Mr. T. Tsuchiya and Dr. Y. Nonomura for suggestive discussions. Thanks are also due to Mr. K. Tsukada for help in projection welding and Ms. A. Inoue for help in device dicing.

(Manuscript received June 16, 1999 revised Sept. 4, 2000)

References

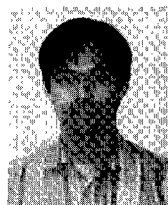
- (1) K. Ikeda, H. Kuwayama, T. Kobayashi, T. Watanabe, T. Nishikawa, T. Yoshida and K. Harada, Silicon pressure sensor integrates resonant strain gauge on diaphragm, *Sensors and Actuators A*, **21-23**, 146-150(1990).
- (2) D. Nicolascu, V. Filip and F. Okuyama, A conceptual design for a microelectronic ionization vacuum gauge, *Appl. Surf. Sci.*, **126 (3-4), Part II**, 292-302(1998).
- (3) Y. Wang and M. Esashi, The structures for electrostatic servo capacitive vacuum sensors", *Sensors and Actuators A*, **66**, 213-217(1998).
- (4) D. D. Bruyker, A. Cozma and R. Puers, A combined piezoresistive/capacitive pressure sensor with self-test function based on thermal actuation, *Sensors and Actuators A*, **66**, 70-75(1998).
- (5) G. N. D. Brabander, G. Beheim and J. T. Boyd, Integrated optical micromachined pressure sensor with spectrally encoded output and temperature compensation, *Appl. Optics*, **37 (15)**, 3264-3267(1998).
- (6) J.-S. Shie, B. C. S. Chou and Y.-M. Chen, High performance Pirani vacuum gauge, *J. Vac. Sci. Technol. A*, **13 (6)**, 2972-2979(1995).
- (7) W. J. Alvesteffer, D. C. Jacobs and D. H. Baker, Miniaturized thin film thermal vacuum sensor, *J. Vac. Sci. Technol. A*, **13 (6)**, 2980-2985(1995).
- (8) N. Fujitsuka, J. Sakata, Y. Miyachi, K. Mizuno, K. Ohtsuka, Y. Taga and O. Tabata, Monolithic pyroelectric infrared image sensor using PVDF thin film, *Sensors and Actuators A*, **66**, 237-243(1998).

Shinan Wang (Non-member) is currently a researcher at Toyota Central R&D Laboratories, Inc. and is devoting to developing micro sensors for practical applications. Before joining Toyota, he was a lecturer at the Venture Business Laboratory in Tohoku University and was engaging in development of micromachining techniques including ceramic micro-processing from Sept. 1996 to Oct. 1998.



He received a B. S. degree in Semiconductor Physics and Devices from Jilin University, Changchun, China, in 1987. He received a M. S. and Ph.D. degree in Electronic Engineering from the University of Tokyo, Japan, in 1992 and 1996. His research interest includes quantum electronic devices and ecologically friendly semiconductor materials and related devices.

Kentaro Mizuno (Non-member) received a B. E. degree in electrical engineering from Meijo University, Nagoya, Japan, in 1989, and an M. E. degree in electronic engineering from Toyohashi University of Technology, Toyohashi, Japan, in 1991, after which he joined Toyota Central Research and Development Laboratories, Inc., Aichi,



Japan. His main research interest is designing analog CMOS integrated circuits for micro-sensors.

Motohiro Fujiyoshi (Member) graduated in 1989 and received his Master degree in mechanical engineering in 1991 from Nagoya University, Nagoya, Japan. He joined Toyota Central Research and Development Laboratories in 1991. As a researcher, he is currently engaging in the development of sensors for automobile.



Hirofumi Funabashi (Non-member) received his B. S. degree from Nagoya Institute of Technology, Nagoya, Japan, in 1982. Since 1982, he has been with Toyota Central Research and Development Laboratories, Inc. He is currently engaged in the research and development of solid-state sensors and surface micromachining process. He is a member of the Japan society of Applied Physics.



Jiro Sakata (Non-member) received the M. S. degree in chemistry from Nagoya University, Nagoya, Japan, in 1978 and the Dr. degree in physical engineering from the University of Tokyo, Tokyo, Japan, in 1989. Since 1978, he has been working for Toyota Central Research and Development Laboratories as a Researcher on thin-film technology.



He is currently Manager of the Advanced Device Laboratory. His research interests are organic and inorganic material science and thin-film technology for sensors and micromachining. Dr. Sakata received the R&D 100 Award for research in "Thin film tensile tester" in 1998.
